

High-resolution electron microscopy of poly(β -hydroxybutyrate)

Jean-François Revol

*Pulp and Paper Research Institute of Canada, Pulp and Paper Building,
McGill University, 3420 University Street, Montreal, PQ, Canada H3A 2A7*

and Henri D. Chanzy*, Yves Deslandes and Robert H. Marchessault†

*Xerox Research Centre of Canada, 2660 Speakman Drive, Mississauga, ON,
Canada L5K 2L1*

(Received 5 December 1988; accepted 24 January 1989)

High-resolution electron microscopy of poly(β -hydroxybutyrate) (PHB) single crystals has allowed direct visualization of the lattice planes of this highly beam-sensitive thermoplastic polyester from bacteria. From lattice images having a resolution of 0.35 nm, a simple Fourier averaging performed optically has generated an image of the crystal projected along its fibre (*c*) axis. The lattice image provides a molecular-level picture of the elliptical PHB cross-section with rows of alternating orientation clearly identifiable, as in the X-ray unit cell packing.

(Keywords: bacterial polyester; single crystals; lattice image; molecular image; low-dose electron microscopy; poly(β -hydroxybutyrate))

INTRODUCTION

New developments in high-resolution, low-dose electron microscopy have led to recent studies reporting electron images obtained at molecular dimensions with synthetic and naturally occurring polymer crystals very sensitive to damage by electron irradiation¹⁻⁸. Such images were proved to be extremely valuable for crystal texture analysis of fibrous polymers⁷, and also, with the help of image processing, for obtaining molecular images along one axis of a crystal⁸.

In the present work, high-resolution, low-dose electron microscopy is performed on poly(β -hydroxybutyrate) (PHB). This naturally occurring optically active polyester is found in the form of 0.5 μ m crystalline granules in the cytoplasmic fluid and constitutes a carbon reserve in a wide variety of bacteria⁹. There have been a significant number of articles published on PHB, most of them reporting on the biological aspects¹⁰, but only a few on the morphology of the native granules^{11,12} and on lamellar single crystals that can be obtained by crystallization from dilute solution¹³⁻¹⁵. In the following, we present lattice imaging of such PHB single crystals, the two major goals being: (i) to obtain, after spatial filtering, images of the molecular packing and to confirm the chain arrangement predicted by the X-ray studies; and (ii) eventually to extend the study to the bacterial copolyester, poly(β -hydroxybutyrate-*co*- β -hydroxyvalerate) (poly(HB-*co*-HV)), which displays isodimorphism¹⁶, i.e. cocrystallization in one or the other of the two homopolymer lattices (depending on composition).

EXPERIMENTAL

Samples of poly(β -hydroxybutyrate) were obtained from ICI, Agricultural Division, Billingham, UK, and are available under the tradename Biopol. Solutions of 0.02 w/w of PHB were heated to 170°C in poly(ethylene glycol) (Carbowax 4000). Once the polymer was completely dissolved, the temperature was lowered to 130°C. After 3 h, crystals had formed. The solution was nevertheless kept at this temperature for an extra 4 h, and then allowed to cool to room temperature. Because of the high viscosity of the poly(ethylene glycol) (PEG), the solution could not be readily filtered.

To avoid damaging the single crystals, a volume of methanol equivalent to the volume of the solution was added to the suspension, which was then allowed to sediment for 24 h. After removing the supernatant liquid and adding an equivalent volume of methanol, the suspension was gently agitated and the suspension was again allowed to sediment. This procedure was repeated 20 times in order completely to remove PEG and to suspend the single crystals in methanol.

Drops of the PHB suspension were deposited on 400-mesh electron microscope grids covered with a 10 nm thick carbon film. The specimens were allowed to dry and were subsequently examined in a Philips EM 400 T electron microscope. This instrument was operated at an accelerating voltage of 120 kV and was equipped with a low-dose unit. Electron micrographs were recorded from never irradiated areas of the grid at a plate magnification of $\times 28\,000$ and with underfocusing conditions of around 100 nm. The illumination conditions were controlled to deliver an accumulated dose of only 100 electrons/nm² to the specimen after an exposure of 2 s. The images were recorded on Ilford (Ilfoset) emulsion and developed for 5 min with Kodak D19 full-strength

* Centre de Recherche sur les Macromolécules Végétales (CNRS), BP 68, 38402 Saint Martin d'Hères Cédex, France

† To whom correspondence should be addressed at McGill University, 3420 University Street, Montreal, Canada H3A 2A7

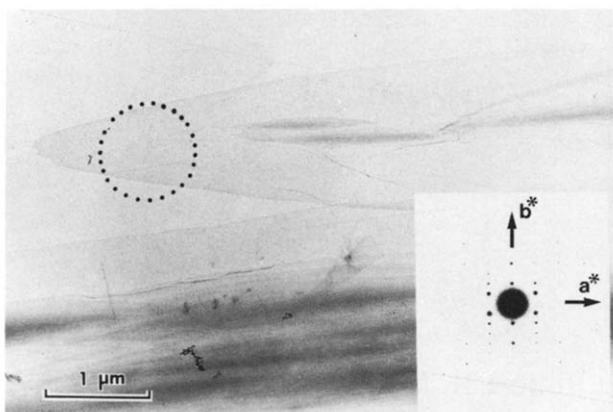


Figure 1 Transmission electron micrograph and its corresponding electron diffractogram of a single crystal of PHB. The circle shows the area from which the electron diffractogram was recorded. The crystal image is properly oriented with respect to the inset diffraction pattern. On the original negative the diffraction spots extended to 0.1 nm resolution

developer. In such conditions the optical density obtained on the photographic plate was about 0.4.

Images were analysed optically by means of a Polaron electromicrograph optical diffractometer. A laser beam was transmitted through a small region of the photograph lattice image and diffracted, as by a grating. The resulting optical diffractograms reveal the periodicities present in the lattice image and the orientation of the specimen. Regions that displayed optical diffraction of the highest resolution and symmetry were selected for further photographic enlargement and image processing.

Fourier filtering was obtained from the previously selected areas. The ray maxima of the optical diffractogram were allowed to pass through a mask having selectively placed holes and located in the diffraction plane. Images were thus reconstructed from those parts of the optical diffractogram that passed through this filter, whose azimuthal position had to be carefully adjusted. In the present work, the filter was made as follows. The optical diffractogram was recorded on a first negative positioned exactly in the diffraction plane. On this negative the maxima of the diffractogram and the central spot were covered by black dots whose diameter just exceeded the diameter of the maxima, i.e. corresponding approximately to 0.01 \AA^{-1} in reciprocal space. By contact printing, a second overexposed negative (black but with totally transparent dots) was produced and used as a mask, which was repositioned in the diffraction plane of the optical bench for further image reconstruction.

RESULTS AND DISCUSSION

A general view of the PHB crystals is presented in *Figure 1*. The crystals are lath-shaped platelets having a lateral dimension of about $1 \mu\text{m}$ and length of $5\text{--}50 \mu\text{m}$. Using metal shadowing, the crystals were found to be about 5 nm thick, where they were transparent, but considerably thicker where they were opaque to the electron beam. Electron diffraction was recorded from selected areas of about $1 \mu\text{m}$ diameter, yielding patterns such as the inset in *Figure 1*. This electron diffraction pattern corresponds to the a^*b^* reciprocal lattice of PHB crystals, the chain axis thus being perpendicular to the

crystal surface. The indexing is consistent with the orthorhombic unit cell previously derived from X-ray diffraction analysis^{17,18} (cell dimensions $a=0.576 \text{ nm}$, $b=1.320 \text{ nm}$, $c=0.596 \text{ nm}$).

A typical high-resolution, low-dose electron micrograph of an individual crystal is shown in *Figure 2*. Evaluation of the micrograph by optical diffraction from a $0.1 \mu\text{m}$ diameter area yielded a diffractogram (insert) showing eight spots organized in a fashion similar to the electron diffraction pattern. This optical diffractogram has a maximum possible resolution of 0.33 nm (040 spacing). But because the observed 040 spot could be a second order of the intense 020, real resolution could be somewhat lower (e.g. corresponding to the 120 spacing, i.e. 0.43 nm). However, when larger areas of about $1 \mu\text{m}$ are selected, the 130 reflection at a spacing of 0.35 nm is observed also (see *Figure 3*). Compared to the original

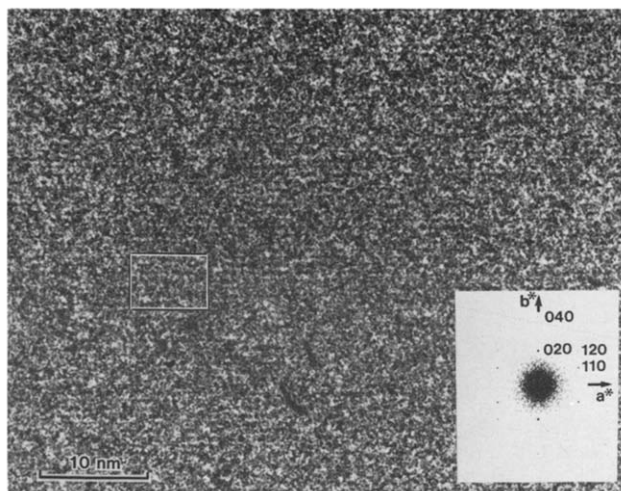


Figure 2 High-resolution, low-dose electron image of PHB showing lattice fringes and the corresponding optical diffraction pattern (inset). In this diffractogram, the background was reduced to a minimum during photographic processing, so that the weakest reflections are just visible. For reference, the reader should note that the 040 reflection corresponds to a d spacing of 0.33 nm. A $0.1 \mu\text{m}$ diameter area was used to produce the optical diffractogram while the ultimate reconstructed image in *Figure 4* corresponds to the rectangular inset area

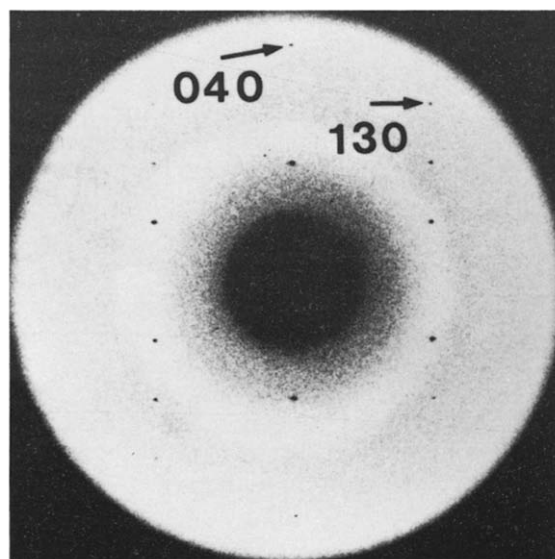


Figure 3 Optical diffraction pattern of a $1 \mu\text{m}$ diameter area of the same micrograph presented in *Figure 2*. Diffraction spots corresponding to the 040 and 130 lattice planes are indicated

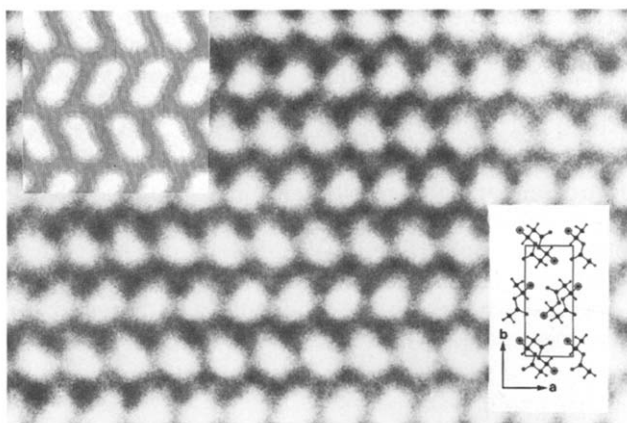


Figure 4 Arrangement of the molecular helices of PHB in the crystal. This image was generated from the image shown in Figure 2, after optical filtering of the $0.1\ \mu\text{m}$ diameter area that produced the optical diffractogram shown in Figure 2. The corresponding area of this filtered image is shown by a rectangular box in Figure 2. Lower right inset: arrangement of the chains in the unit cell according to Cornibert *et al.*¹⁷. The largest circles correspond to the CH_3 groups and the smallest to the hydrogens; carbon and oxygen are shown as full black dots. Upper left inset: PHB image simulation²⁰ calculated with $\lambda = 0.003\ 349\ \text{nm}$, $C_s = 2.8\ \text{mm}$ and with an objective aperture corresponding to $0.3298\ \text{nm}$. The underfocus value was $\Delta f = 110\ \text{nm}$

negative of the electron diffractogram shown in Figure 1 (resolution $0.1\ \text{nm}$), there is a significant degradation in resolution as a result of the electron imaging process. Lattice lines corresponding to the (020) planes can be seen directly on the image. Other lattice lines are only revealed by optical diffraction because of the high noise level present in this image.

Because the image was recorded at a relatively low magnification ($\times 28\ 000$) the grain size of the photographic emulsion used is of the order of the resolution obtained, which is one reason for the poor-quality image. In addition, the very low exposure dose used, i.e. $100\ \text{e}^-/\text{nm}^2$, is far less than the electron dose required to produce a statistically well defined image and a high level of 'random noise' is produced. The resulting image appears to have little structural information other than the presence of the (020) fringes.

For such crystalline substrates, however, the molecular structure is periodically repeated over relatively large distances. Averaging techniques or summation procedures can thus overcome the low signal-to-noise limitation, and a picture can be constructed from the fragmented information. Spatial averaging by Fourier filtration is a well known technique for that purpose and can be performed optically or by computer. In the optical diffractogram that represents the first Fourier transform, all the information coming from the crystal structure is concentrated in the maxima, the remainder being the contribution of random noise. Thus, a second Fourier transform on the filtered diffractogram, as described in the 'Experimental' section, allows reconstruction of the image, without noise interference. If the windows in the mask are just large enough to allow the ray maxima to pass through, as in the present work, a spatial averaging is also obtained¹⁹. Figure 4 shows such an optically reconstructed image. Individual chains seen along the c axis are clearly indicated by white ellipsoids. A molecular projection according to the known X-ray crystal structure¹⁷ is inset for comparison. There is good agreement between the model and the filtered electron image. In

particular, the general shape and the setting angle of the molecules with respect to the unit cell are in close resemblance with the model, even though the resolution does not reveal atomic details.

Mention should be made here that images such as the one presented in Figure 4 and obtained by optical Fourier filtration of areas of about $0.1\ \mu\text{m}$ diameter on the original micrograph extend uniformly over distances exceeding $20\ \text{nm}$ (Figure 5a). On the other hand, when only the noise is allowed to pass through the mask the reconstructed images (such as in Figure 5b) are periodic but with a random intensity distribution. This randomness, with frequent reversals of contrast, is created by the white noise that passed through the mask. Thus, the filtered images shown in Figures 4 and 5a do not represent the reconstruction of the noise, which would have been artificially biased by the diffraction mask, but the reconstruction of the structural information that is contained in the maxima of the optical diffractogram.

In order to evaluate the contribution of the weakest reflections (120 and 040) to the filtered image, optical diffractograms were recorded from a magnified negative corresponding to an area of about $20\ \text{nm}$, within the larger region ($0.1\ \mu\text{m}$) used for optical filtration of Figure 4. The patterns exhibit very weak 120 and 040 reflections, just visible above the noise level. Further, when a smaller area of about $4\ \text{nm}$ is selected, the 120 reflection is no longer detected, and although the 040 reflection is still present, as seen in Figure 6, it is highly probable that these weakest reflections cannot contribute significantly to the optically filtered image. Obviously, in this case, the noise passing through the mask openings is dominant. In order to verify this assumption, an image was also reconstructed with only the intense 020 and 110 reflections. The final image obtained was essentially the same as in Figure 4, showing that, although the original image contains information at a resolution of at least $0.35\ \text{nm}$ (130 reflection), the optical filtered image might have a lesser resolution, e.g. as low as $0.528\ \text{nm}$ (110 reflection).

Finally, it should be mentioned here that the exact defocus value of the objective lens has not been measured by means of the usual optical diffraction of the supporting carbon film. Indeed, statistical noise coming from the low electron dose used as well as the emulsion grain ($0.3\text{--}0.7\ \text{nm}$ at the magnification used in the present work) mask the first zeros of the phase-contrast transfer function

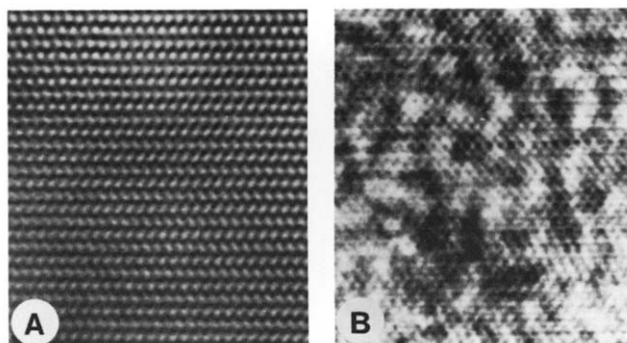


Figure 5 Optically filtered image obtained as in Figure 4, but corresponding to another region at a lower magnification. (A) The ray maxima of the optical diffractogram passed through the mask openings. (B) The ray maxima of the optical diffractogram were stopped by the mask and only random noise was allowed to pass through the openings

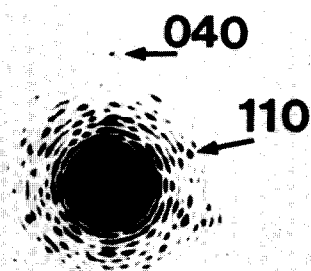


Figure 6 Optical diffraction pattern obtained from a 4 nm diameter area of the micrograph presented in Figure 2. Note the 040 reflection at 0.33 nm spacing

of our microscope (at the Scherzer focus the first zero is at 0.37 nm). Knowledge of this defocus value is, however, crucial in order to know if the image obtained is the real representation of the crystal structure. Therefore, the correspondence of the reconstructed image to the actual crystal structure was also verified by a kinematic image simulation performed at various defocus values Δf of the objective lens²⁰. A perfect match was obtained at $\Delta f = 110$ nm underfocus, which is close to the Scherzer focus. Such a simulated image is presented as an inset in Figure 4.

CONCLUSIONS

The result presented in this paper demonstrates that PHB can be successfully analysed by high-resolution electron microscopy, in spite of the electron beam sensitivity of this material. More specifically, lattice imaging at a resolution of at least 0.35 nm was obtained and the image

of the crystal projected along its fibre (c) axis was generated at a molecular level by a simple Fourier averaging performed optically. Improvements of this image should be possible by using the image enhancement method described elsewhere⁴. In addition, because of the richness of the electron diffractogram, it is possible that more details at higher resolution could be obtained. Since it is possible to grow single crystals of the crystalline copolyester, poly(HB-co-HV), this may allow direct detection of lattice faults and strains, which are believed to be associated with the isodimorphism reported for these materials¹⁶.

REFERENCES

- 1 Sugiyama, J., Harada, H., Fujiyoshi, Y. and Uyeda, N. *Mokuzai Gakkaishi* 1984, **30**, 98
- 2 Revol, J. F. *J. Mater. Sci. Lett.* 1985, **4**, 1347
- 3 Revol, J. F. and St John Manley, R. *J. Mater. Sci. Lett.* 1986, **5**, 249
- 4 Chanzy, H., Folda, T., Smith, P., Gardner, K. and Revol, J. F. *J. Mater. Sci. Lett.* 1986, **5**, 1045
- 5 Revol, J. F. and Chanzy, H. *Biopolymers* 1986, **25**, 1599
- 6 Chanzy, H., Smith, P. and Revol, J. F. *J. Polym. Sci., Polym. Lett. Edn.* 1986, **24**, 557
- 7 Chanzy, H., Smith, P., Revol, J. F. and St John Manley, R. *Polym. Commun.* 1987, **28**, 133
- 8 Revol, J. F., Gardner, K. H. and Chanzy, H. *Biopolymers* 1988, **27**, 345
- 9 Doudoroff, M. and Stanier, R. *Nature* 1959, **183**, 1440
- 10 Williamson, D. H. and Wilkinson, J. F. *J. Gen. Microbiol.* 1958, **19**, 198
- 11 Alper, R., Lundgren, D. G., Marchessault, R. H. and Cote, W. A. *Biopolymers* 1963, **1**, 545
- 12 Ellar, D., Lundgren, D. G., Okamura, K. and Marchessault, R. H. *J. Mol. Biol.* 1968, **35**, 489
- 13 Barenberg, S. A., M.Sc. Thesis, Case Western Reserve University, 1971
- 14 Marchessault, R. H., Coulombe, S., Morikawa, H., Okamura, K. and Revol, J. F. *Can. J. Chem.* 1981, **59**, 38
- 15 Barham, P. J., Keller, A., Otum, E. L. and Holmes, P. A. *J. Mater. Sci.* 1984, **19**, 2781
- 16 Bluhm, T. L., Hamer, G. K., Marchessault, R. H., Fyfe, C. A. and Veregin, R. *Macromolecules* 1986, **19**, 2871
- 17 Cornibert, J. and Marchessault, R. H. *J. Mol. Biol.* 1972, **71**, 735
- 18 Yokouchi, M., Chatani, Y., Tadokoro, H., Teranishi, K. and Tani, H. *Polymer* 1973, **14**, 267
- 19 Misell, D. L. in 'Image Analysis, Enhancement and Interpretation', North-Holland, Amsterdam, 1978
- 20 Tsuji, M., personal communication